STAR Protocols

CellPress
OPEN ACCESS

Protocol

Laser microirradiation as a tool to investigate the role of liquid-liquid phase separation in DNA damage repair

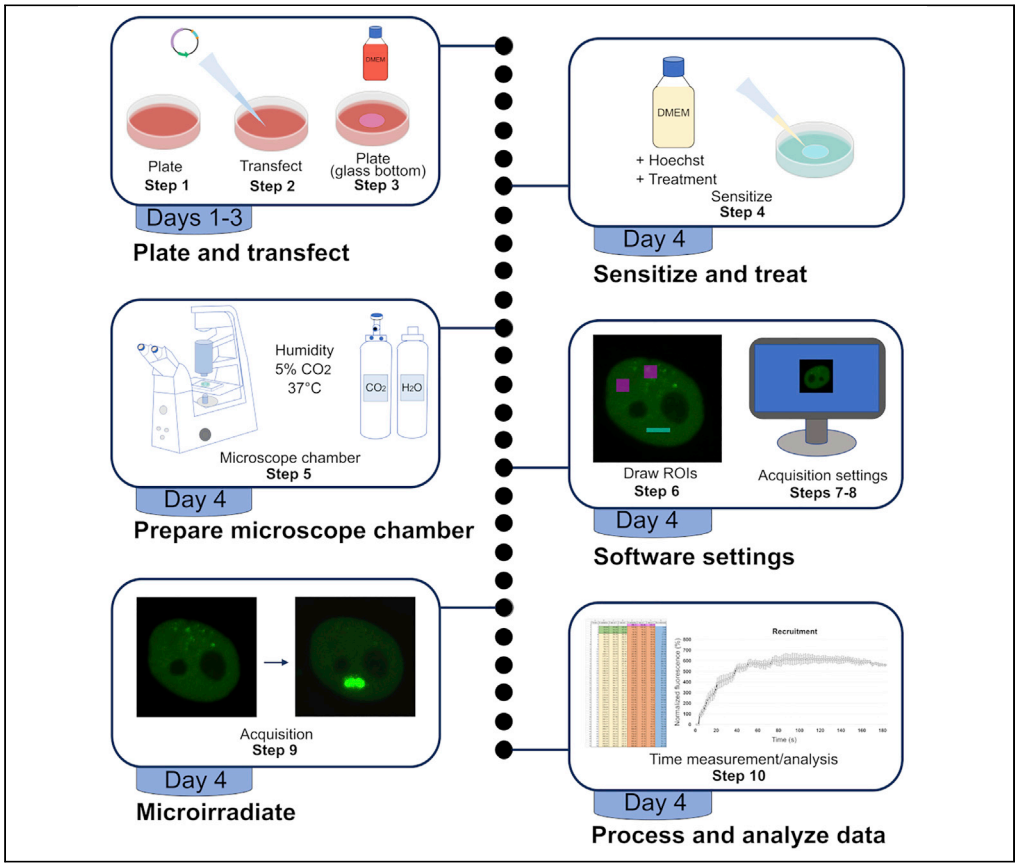

Here we describe a protocol for the generation of site-specific DNA damage, including double and single strand breaks, using the 405 nm laser of a confocal microscope in cells pre-sensitized with Hoechst. This is a simple approach, particularly useful to assess the involvement of proteins and the roles of liquid-liquid phase separation in DNA damage repair. Examples of transfection protocol, drug concentrations, and microscopy are provided, although optimization may be needed for specific experimental setups and cell lines used.

Brunno Rocha Levone, Silvia Lombardi, Silvia M.L. Barabino

brunno.rochalevone@unimib.it (B.R.L.)
silvia.barabino@unimib.it (S.M.L.B.)

Highlights

Protocol for the generation of site-specific DNA damage in living cells

Using a 405 nm laser of a confocal microscope in pre-sensitized cells

Analysis of the kinetics of proteins in DNA damage repair

Analysis of the roles of liquid–liquid phase separation in DNA damage repair

Levone et al., STAR Protocols 3, 101146
March 18, 2022
https://doi.org/10.1016/j.xpro.2022.101146

STAR Protocols

CellPress
OPEN ACCESS

Protocol

Laser microirradiation as a tool to investigate the role of liquid-liquid phase separation in DNA damage repair

Brunno Rocha Levone,[1,2,3,*] Silvia Lombardi,[1,2] and Silvia M.L. Barabino[1,4,*]

[1]Department of Biotechnology and Biosciences, University of Milano-Bicocca, 20125 Milan, Italy

[2]These authors contributed equally

[3]Technical contact

[4]Lead contact

*Correspondence: brunno.rochalevone@unimib.it (B.R.L.), silvia.barabino@unimib.it (S.M.L.B.)
https://doi.org/10.1016/j.xpro.2022.101146

SUMMARY

Here we describe a protocol for the generation of site-specific DNA damage, including double and single strand breaks, using the 405 nm laser of a confocal microscope in cells pre-sensitized with Hoechst. This is a simple approach, particularly useful to assess the involvement of proteins and the roles of liquid-liquid phase separation in DNA damage repair. Examples of transfection protocol, drug concentrations, and microscopy are provided, although optimization may be needed for specific experimental setups and cell lines used.

For complete details on the use and execution of this protocol, please refer to Levone et al. (2021).

BEFORE YOU BEGIN

Here, we describe a protocol for the generation of DNA damage using a 405 nm laser, commonly present in any confocal microscope. This method is useful for assessing the spatiotemporal dynamics of protein recruitment at DNA damage sites in living cells, and we used it to study the role of liquid-liquid phase separation (LLPS) in DNA damage repair.

Optimize transfection protocol and microscope settings

Timing: 3–7 days

1. Plate and perform transient transfections with the DNA plasmids expressing each protein of interest fused to a fluorescent protein (e.g., EGFP, YFP, RFP or mCherry) in the cell line of choice.
2. Observe transfected cells 24–48 h with a fluorescence microscope. Correct cellular localization, protein expression levels and cell heath should be considered when optimizing the transfection protocol.

   Note: We used HeLa cells, transfected with Lipofectamine 2000. However, a different transfection protocol and other adherent mammalian cell lines, such as C2C12 and U2OS, can be used. We also successfully applied this protocol with minor changes to HEK293 cells.

   Alternatives: In alternative to transient transfections, stably transfected cells have also been previously used (Mortusewicz et al., 2008, Tsukada et al., 2021).

3. Once the transfection protocol is optimized, check your microscope settings, including laser power output. Perform a pilot experiment to determine the specific laser power able to generate DNA damage and induce protein recruitment.

a. Fix and perform immunofluorescence in irradiated cells to assess, for example, the phosphorylation of H2AX.
b. Use control proteins and assess their recruitment. KU80 and NBS1 are recruited to double strand breaks, and PARP1 and XRCC1 are recruited to single strand breaks.

Note: As the transfected cells will be fluorescent, note that any control immunofluorescence should be done using a secondary antibody of a color different from that of the fluorescent protein.

KEY RESOURCES TABLE

REAGENT or RESOURCE	SOURCE	IDENTIFIER
Experimental model: Cell lines		
HeLa WT cells	ECACC	Cat#93021013
HEK293 WT cells	ECACC	Cat#85120602
Recombinant DNA		
KU80-GFP plasmid	Britton et al. (2013)	Addgene Cat#46958
NBS1-GFP plasmid	A. Nussenzweig	N/A
FUS-GFP plasmid	Cloned in house	N/A
53BP1-GFP plasmid	Fradet-Turcotte et al. (2013)	Addgene Cat#60813
XRCC1-RFP plasmid	M. Cristina-Cardoso	N/A
Antibodies		
Rabbit anti-γH2AX (1:200)	Cell Signaling Technology	Cat#9718S
Mouse anti-γH2AX (1:200)	Cell Signaling Technology	Cat#80312S
Rabbit anti-Coilin (1:100)	Homemade	Prof. Lamond
Mouse anti-SC35 (1:100)	Sigma-Aldrich	Cat#S4045
Alexa Fluor 488 goat anti-rabbit	Invitrogen	Cat#A-11008
Alexa Fluor 647 goat anti-mouse	Invitrogen	Cat#A-21235
Software and algorithms		
NIS-Elements	Nikon	https://www.microscope.healthcare.nikon.com/products/software/nis-elements
Excel	Microsoft	https://www.microsoft.com/en/microsoft-365/
Others		
DMEM High Glucose	Sigma-Aldrich	Cat#D5796
Fetal Bovine Serum	EuroClone	Cat#ECS0180L
Penicillin-Streptomycin	Sigma-Aldrich	Cat#P4333
L-Glutamine	Sigma-Aldrich	Cat#G7513
Trypsin-EDTA	EuroClone	Cat#ECB3052D
Lipofectamine 2000	Invitrogen	Cat#11668019
OptiMEM	Invitrogen	Cat#11058021
DMEM High Glucose Phenol red-free	Sigma-Aldrich	Cat#D1145
Hoechst 33342	Sigma-Aldrich	Cat#B2261
Paraformaldehyde (PFA)	Sigma-Aldrich	Cat#P6148
1,6-Hexanediol	Sigma-Aldrich	Cat#240117
2,5-Hexanediol	Sigma-Aldrich	Cat#H11904
Ammonium acetate	Merck	Cat#1.01116
Bis-ANS dipotassium salt	Sigma-Aldrich	Cat#D4162
Syringe filter 0.22 μm pore size	Several suppliers	N/A
Sterile syringe 10 mL	Several suppliers	N/A
Petri dish 3.5 cm diameter	Corning	Cat#353001
Petri dish with glass bottom 3.5 cm diameter	Thermo Scientific	Cat#150680
Attofluor® cell chamber	Invitrogen	Cat#A-7816

(*Continued on next page*)

Continued

REAGENT or RESOURCE	SOURCE	IDENTIFIER
Nunc™ Lab-Tek™ chambered coverglass #1	Thermo Scientific	Cat#155383PK
Confocal Microscope Nikon Eclipse Ti A1-A	Nikon	N/A
Microscope incubator	Oko Lab	Cat#H101-K-FRAME
Immersion oil for fluorescence microscopy	Nikon	Cat#MXA22168

MATERIALS AND EQUIPMENT

Plasmids should be highly pure (A_{260}/A_{280} 1.7–1.9; A_{260}/A_{230} 2.0–2.2) and almost exclusively in the supercoiled form to ensure optimal transfection. The supercoiled plasmid should appear as the predominant and fastest band in agarose gel electrophoresis. Reduced supercoiled plasmid may result from excessive lysis during purification or from frequent freeze-thaw cycles. To avoid plasmid denaturation, do not exceed the lysis time (according to the purification kit used) and aliquot the plasmid to avoid excessive freeze-thaw cycles. The concentration to be used for transfection will depend on the expression level of the target protein but should allow low level expression to reduce artefacts. All drugs should be freshly diluted before the beginning of the experiments. We prepared the stock dilutions as below:

- Hoechst: 1 mg/mL, diluted in water (sterile filter after dilution with a 0.22 μm syringe filter), 50 μL aliquots kept at −20°C;
- Paraformaldehyde (PFA): 4%, diluted in PBS (pH 7.4), 15 mL aliquots kept at −20°C;
- Ammonium acetate: 7.63 M, diluted in water (sterile filter after dilution with a 0.22 μm syringe filter), 2 mL aliquots kept at 18°C–22°C.

Reagent	Final concentration	Amount
Cell culture medium for cell growth		
DMEM High Glucose	n/a	500 mL
FBS	10%	56 mL
Penicillin-Streptomycin	1%	5.6 mL
Total	n/a	561.6 mL
Cell culture medium for microirradiation		
DMEM Phenol red-free	n/a	17.6 mL
FBS	10%	2 mL
Penicillin-Streptomycin	1%	200 μL
L-Glutamine	1%	200 μL
Hoechst	0.5 μg/mL	10 μL
Total	n/a	20 mL

The 1,6-Hexanediol (1,6-HD) and 2,5-Hexanediol (2,5-HD) are aliphatic alcohols used to study LLPS. While 1,6-HD impairs LLPS, 2,5-HD is used as a negative control, as it is a less hydrophobic isomer and does not affect LLPS. 1,6-HD and 2,5-HD were added directly to the cell culture medium prior to cell treatment. Their concentration is indicated by %, which represents g of Hexanediol for each 100 mL of the final volume.

⚠ CRITICAL: Hoechst (a DNA intercalant) and PFA (moderately toxic by skin contact and inhalation) should be handled with special care. 1,6-Hexanediol, 2,5-Hexanediol and ammonium acetate have low toxicity levels but may irritate mucous membranes if inhaled.

Alternatives: Some protocols may use other intercalants to sensitize the DNA to the 405 nm laser-induced damage. These alternatives include incubating cells with 10 μM Bromodeoxyuridine (BrdU) for 24 h prior to microirradiation (BrdU should also be handled with care). Due to the limited solubility of BrdU in water and the longer time needed for sensitization, we opted

for Hoechst instead. Moreover, Hoechst is fluorescent, and allows visualization of the nuclei while performing microirradiation, if necessary.

Equipment

The confocal microscope used for this experiment should be equipped with at least two lasers, the 405 nm for the microirradiation, and another (such as 488 or 560 nm) for the imaging. Our 405 nm laser used for microirradiation has a total power output of 405.7 mW. To guarantee that living cells are healthy and to avoid unnecessary oxidative damage, it is strongly recommended that the microscope should be equipped with an incubation chamber for the regulation of the humidity and CO_2 levels.

STEP-BY-STEP METHOD DETAILS

Cell transfection and plating onto glass-bottom dishes

Timing: 3 days

To obtain cells expressing fluorescent-tagged proteins, cells are transiently transfected using transfection reagents. Transfected cells will then be used in the next major step.

1. Trypsinize, count and plate 200,000 HeLa cells per well onto 6-well plates or 3.5 cm Petri dishes in cell culture medium.
   a. If cells do not grow at same pace (e.g., in the comparison between wild type and knockout cells), an optimization will be needed for the ideal number of cells to be plated for each cell line.
2. From 18 to 24 h after plating, transfect cells using ~ 1 μg plasmid DNA and 2–3 μL Lipofectamine 2000 (both diluted in OptiMEM to a final volume of 500 μL).
3. From 18 to 24 h after transfection, trypsinize, count and plate 100,000 transfected cells onto glass-bottom 3.5 cm Petri dishes (to aid cell adhesion, coating with poly-D-lysine or laminin could be applied if necessary).

   Alternatives: To avoid having to trypsinizing cells twice and save time, cells can be plated and transfected directly onto glass-bottom Petri dishes. If this alternative is used, number of cells to be plated and transfection protocol should be optimized. For optimal cell imaging, allow cells to express GFP-tagged proteins for at least 36–48 h after transfection.

   Note: For these experiments, we used homemade Petri dishes with glass bottom, by drilling the bottom of a commercial dish, gluing a glass coverslip using a non-toxic silicone, and sterilizing with UV light for at least 30 min. We also performed this experiment using Petri dishes already containing a glass bottom, which are commercially available (see key resources table).

   Alternatives: Chambered slides can also be used (see key resources table), but these should have a glass bottom and the optical characteristics required for confocal imaging. Transfected cells attached to a loose coverslip can also be used coupled to an Attofluor® cell chamber (Invitrogen, see key resources table).

Classical laser microirradiation experiment

Timing: 60–120 min

Transfected cells expressing fluorescent-tagged proteins are microirradiated and the protein recruitment to DNA damage sites is assessed in a time- and site-specific manner.

4. The day after plating the transfected cells onto glass-bottom Petri dishes, prepare cell culture medium for microirradiation (see recipe in materials and equipment section).

a. Add 0.5 μg of Hoechst per milliliter of culture medium (1:2000 dilution from the stock described above).
b. Remove the medium from the Petri dish and add 2 mL of phenol-red free medium containing Hoechst.

Note: Cell should be sensitized with Hoechst for 30 min prior to the initiation of the laser microirradiation in the microscope chamber at 37°C with 5% CO_2.

Note: For setting this protocol, we used a Nikon Eclipse Ti A1-A confocal microscope and the acquisition software NIS-Elements. Screenshots of the steps to be followed are shown in Figure 1. Settings could vary in different devices or software.

5. While cells are being sensitized inside the microscope chamber, turn on the confocal microscope, the 405 nm laser (which in our microscope has a total power output of 405.7 mW) and the acquisition software.

⚠ CRITICAL: To avoid oxidative damage, cells should be maintained in a humidified chamber at 37°C and 5% CO_2 (for 0.6 L/min of air flow, set 0.03 L/min of CO_2 flow). Although not mandatory, the medium containing Hoechst can be removed and changed with fresh phenol red-free medium 30 min after sensitization to avoid excessive sensitization.

6. As shown in Figure 1, each experiment comprises the sequential irradiation of three cells.
   a. Go to the live imaging screen.
      i. Add 3 rectangular Regions of Interest (ROIs).
      ii. Add 7 square ROIs.
   b. Set the rectangular ones as "Bleaching ROIs", which should be 5 pixels in height and variable length.
   c. Six of the square ROIs are used for bleaching control of imaging overtime, and one is used as the background control. Their size can be variable, depending on the cell size and space between them. Avoid placing a ROI over nucleoli or intense GFP granules.
7. We used a 60× objective (numerical aperture of 1.4, oil objective) with 5× digital zoom.
   a. Set image resolution to 512 × 512-pixels (lower resolution), if assessing one picture per second, or 1024 × 1024-pixels (higher resolution), if assessing less timepoints (ex. one picture every 30 s).
   b. Set scan speed to Fast: 2 frame/s (pixel dwell 0.7 μs) for 512 × 512-pixels images or 0.5 frames/s (pixel dwell 1.1 μs) for 1024 × 1024-pixels images.
   c. Set count to 2 (line average of two images is performed for each timepoint).
   d. Go to "Photo Activation/Bleaching" page.
      i. Select only the 405 nm laser, setting 5%–25% as the laser power (power 20.3–101.4 mW).
      ii. Select Keep HV as the HV mode during stimulation and HV linear correction.
      iii. Select the same settings for the other stimulation area in case multiple cells are to be irradiated at once.
      iv. Still on that page, set scan speed to 4 s per frame (pixel dwell 12.4 μs).

Note: The "HV Linear Correction" is used to avoid the steep gain variation that occurs beyond a certain HV point; this function corrects the gain variation to the same rate as the HV adjustment. The "HV mode during stimulation" dictates whether the detector gain should be set to zero during the stimulation phase to avoid detector overload. By choosing "Keep HV" as the HV mode during stimulation, a stable gain will be assured in the subsequent acquisition phase, as the detector gain could drift if turned off and on again.

⚠ CRITICAL: The laser power will affect the amount and type of DNA damage caused. This value should be optimized by the user, by observing the recruitment of control proteins and/or fixing cells and doing immunofluorescence control for γH2AX.

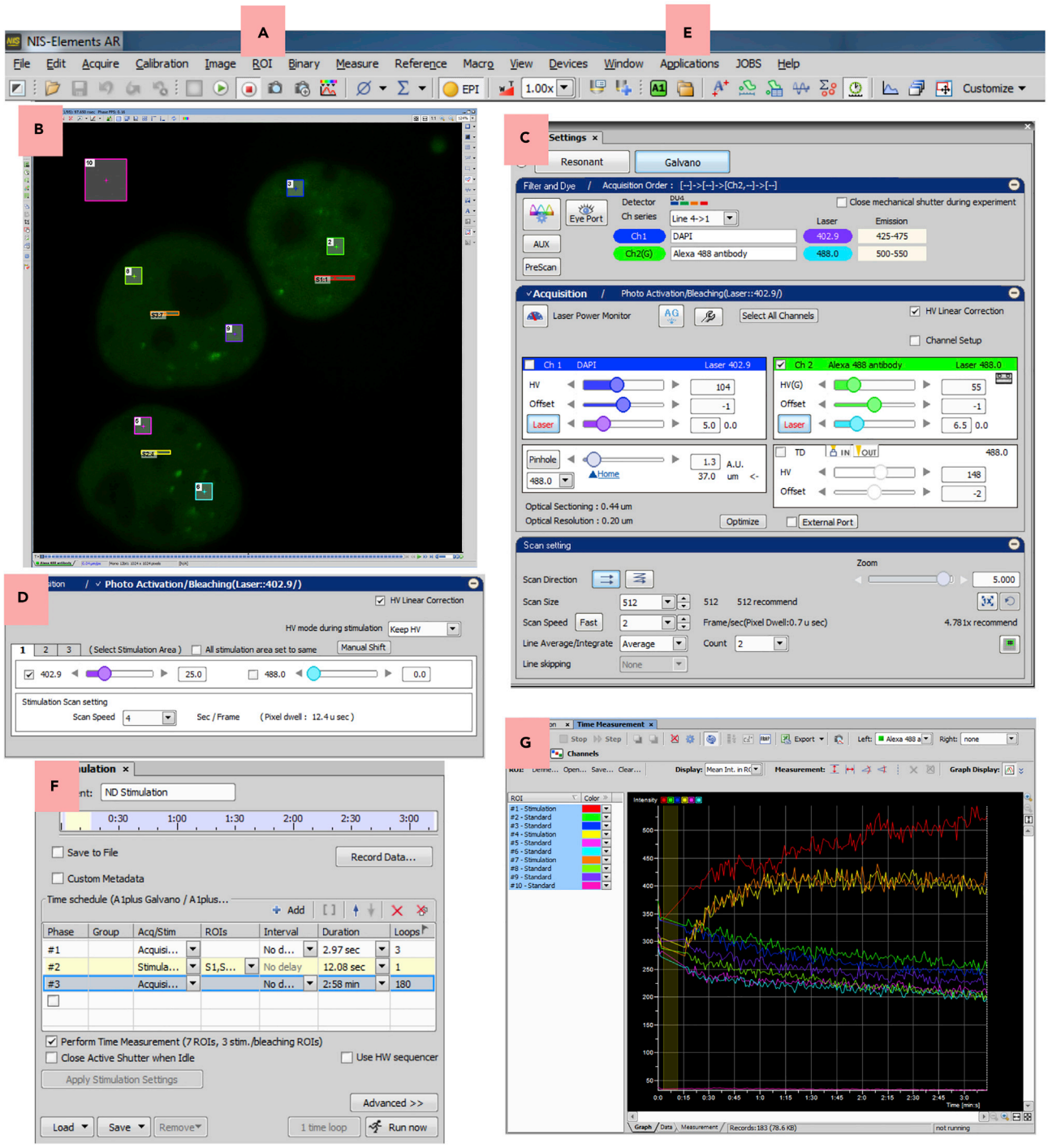

Figure 1. Walkthrough of the NIS-Elements software for guidance

(A) select "ROI" and draw seven square ROIs and three rectangular ones.

(B) Right click the rectangular ROIs and set them to "Bleaching ROIs". Adjust their size, bleaching ROIs height should be set to 5 pixels.

(C) in "Acquisition", select the desired brightness. In "Scan setting", set "Scan Size" to 512 × 512-pixels or 1024 × 1024-pixels, "Scan speed" to fast, "Count" to 2 and "Zoom" to 5.

(D) Near the acquisition tab, click the "Photo Activation/Bleaching" tab and select the 405 nm laser, setting its power to 5–25%. Select "Keep HV" as "HV mode during stimulation" and "Scan Speed" to 4 s per frame (pixel dwell 12.4 μs).

(E) Select "Applications" and "ND stimulation".

Figure 1. *Continued*
(F) In the "ND stimulation" tab, define three phases, one Acquisition (3 loops, to take three baseline images), one Stimulation (select all stimulation ROIs, only 1 loop), and another Acquisition (select the number of images to be taken and the interval between them; in this example, 180 images are taken within 3 min, which means one image per second). Still in this window, select "Perform Time Measurement" and "Apply Stimulation Settings" and click "Run now".
(G) the "Time Measurement" tab will open and display the ROIs mean fluorescence. Once the irradiation is finished, save the file, and click export to and Excel table.

8. Open the ND setup window and set the experiment to have 3 phases: acquisition (pre-irradiation), stimulation (irradiation) and acquisition (post-irradiation).
   a. Set the first acquisition to three and the stimulation to one, whereas the second acquisition phase is variable, depending on how long the acquisition should be, and whether photos are to be taken every second or with which interval.

   Note: The number of images taken after irradiation and interval between them will define the total time of acquisition. For apical proteins (e.g. KU80), we acquire images for 3 min (one photo per second), for other proteins (e.g. FUS) we use 5 min (one photo every 30 s) and for downstream/effector proteins (e.g. 53BP1) we use 15 min acquisition (one photo every minute). Longer acquisitions may result in cells moving [see troubleshooting 2].

9. Once all ROIs are in place, click "Apply Stimulation Settings", click "Run now" and wait the end of the acquisition. No photos will be taken during the irradiation phase, which should take approximately 4 s for a single cell irradiation and 12 s for 3 cells irradiation (see Methods video S1 for an example and Methods video S2 for troubleshooting).

   ⚠ CRITICAL: Cell should be sensitized with Hoechst for 30 min prior to the initiation of the laser microirradiation experiment and can be used until approximately 60 min from the addition of Hoechst. Each Petri dish can be used for 5–6 aquisitions, if using a 3 min protocol. If several cells need to be acquired, we recommend plating more Petri dishes. Use the same laser power across different replicates of each experiment.

   Note: In our microscope setting, we can define up to three "Bleaching ROIs". However, the irradiation is sequential, that is, the irradiation takes place in one cell at a time. For proteins that are recruited at later time points, this is not a problem, but for proteins that are recruited very early, i.e., within a few seconds from irradiation, it would be better to select just one "Bleaching ROI" and irradiate only one cell at a time.

10. After finishing the acquisition, perform "Time measurement" (this can also be done simultaneously with the acquisition), export data and proceed to data analysis.

    Note: To demonstrate that the laser microirradiation protocol successfully induced the formation of DSBs, some Petri dishes containing irradiated cells should be fixed with 4% PFA immediately after irradiation. Cells should then be stained for γH2AX or another DNA damage marker (such as pATM, etc) using a standardized immunofluorescence protocol. As mounting is not possible, we recommend that cells should be imaged immediately after staining. If this is not possible, dishes can be filled with PBS to make sure cells do not dry out and kept in fridge covered with aluminum foil for the shortest period of time.

Laser microirradiation as a tool to investigate the role of liquid-liquid phase separation in DNA damage repair

To study whether the liquid-liquid phase separation (LLPS) is necessary for the recruitment of DNA damage factors, we have used compounds that perturb LLPS, 1,6-Hexanediol (1,6-HD) and Ammonium acetate (Am. Ac.). 1,6-HD is an aliphatic alcohol that dissolves various cytoplasmic and nuclear membraneless compartments *in vivo* by disrupting hydrophobic interactions (Allodi et al., 2016; Kroschwald et al., 2015; Updike et al., 2011; Yamazaki et al., 2018), and partially dissolves FUS

polymers *in vitro* (Allodi et al., 2016; Kato and McKnight, 2018). 2,5-Hexanediol (2,5-HD) is a less hydrophobic isomer of 1,6-HD that does not affect LLPS (Allodi et al., 2016; Kato and McKnight, 2018), and can thus be used as a negative control. Am. Ac. is a hygroscopic salt that inhibits RNA-protein gelation without perturbing intracellular pH (Hamaguchi et al., 1997; Jain and Vale, 2017)ì. It leads to the disappearance of nuclear CAG-repeat RNA foci and ribonucleoprotein bodies that depend on ionic interactions (Jain and Vale, 2017), and was recently shown to rapidly dissolve 53BP1 foci (Pessina et al., 2019). Additionally, bis-ANS is a small molecule that was recently shown to promote a biphasic control of phase separation, while low concentrations strongly promote LLPS, higher concentrations disrupt liquid droplets (Babinchak et al., 2020), and can thus be tested as a potential drug to be used in microirradiation experiments.

To perform a laser microirradiation experiment in the presence of these drugs that interfere with LLPS, simply add the drugs together with Hoechst in step 4 from the previous protocol. Specifically, remove the medium from the Petri dish and add 2 mL of phenol-red free medium containing both the treatment of choice, and Hoechst. For the aliphatic alcohols, a 2% concentration is enough to disrupt phase separation, but mild enough to allow HeLa cells to recover after its withdrawal (Levone et al., 2021). For ammonium acetate, both 50 or 100 mM can be used; while 50 mM cause a mild effect in LLPS in HeLa cells, 100 mM is stronger, but may also compromise cell health in certain cell lines. Although little has been described regarding the use of the small molecule bis-ANS, Babinchak and collaborators described that high concentration disrupt phase separation *in vitro* (Babinchak et al., 2020). If using bis-ANS, note that it is a fluorescent molecule (detected between 410 and 490 nm wavelengths).

> *Note:* To demonstrate that the specific drug concentrations are enough to disrupt LLPS, a validation by immunofluorescence is necessary.

EXPECTED OUTCOMES

This protocol is meant to be used as a tool to study the recruitment of proteins to DNA damage sites generated by irradiation with a 405 nm laser, commonly present in any confocal microscope. It is important to note that multiple types of DNA damage can be induced by microirradiation with the 405 nm laser, including double strand breaks (DSBs), single strand breaks (SSBs) and oxidized bases (Muster et al., 2017). We have recently used this protocol to show that HeLa cells bearing a knockout of the *FUS* gene display changes in the recruitment of proteins related to both nonhomologous end joining (NHEJ) and homologous recombination (HR) repair pathways of DSBs (Levone et al., 2021). Protocols for the generation of specific DNA lesions (DSBs or SSBs) may require more specific equipment, such as UV-A (337–355 nm) or femtosecond near-infrared (800 nm) lasers (Kong et al., 2009). With this protocol, it is possible to assess not only whether a protein of interest accumulates at DNA damage sites, but also whether the silencing or the knockout of a gene, or the pre-treatment of cells with a specific compound can affect the recruitment of the protein of interest. While some proteins are apical in the cascade of DNA damage repair and are recruited in the first seconds upon microirradiation, downstream proteins require a longer acquisition time, as they are only recruited several minutes after microirradiation. Figure 2 shows examples of the recruitment of proteins to microirradiation sites, such as KU80 (Figure 2A) and NBS1 (Figure 2B), that are key apical proteins of the nonhomologous end joining and homologous recombination repair pathways, respectively; and 53BP1 (Figure 2C), an effector protein of the nonhomologous end joining repair pathway. Using a femtosecond near-infrared laser for the induction of DSBs, Saquilabon Cruz and collaborators (Saquilabon Cruz et al., 2016) found that the lowest power for the detection of 53BP1 recruitment was 25 mW, while the recruitment of other proteins required a power higher than 85 mW. In our protocol, we recommend using a 405 nm laser power ranging from 20.3 to 101.4 mW. To confirm that even 5% laser (20.3 mW) can induce the formation of DSBs, HeLa cells transfected with FUS-GFP were microirradiated, fixed with 4% PFA, and stained for γH2AX (red), a known marker of DSBs. In Figure 2D, we can observe that FUS-GFP accumulates at DSBs sites.

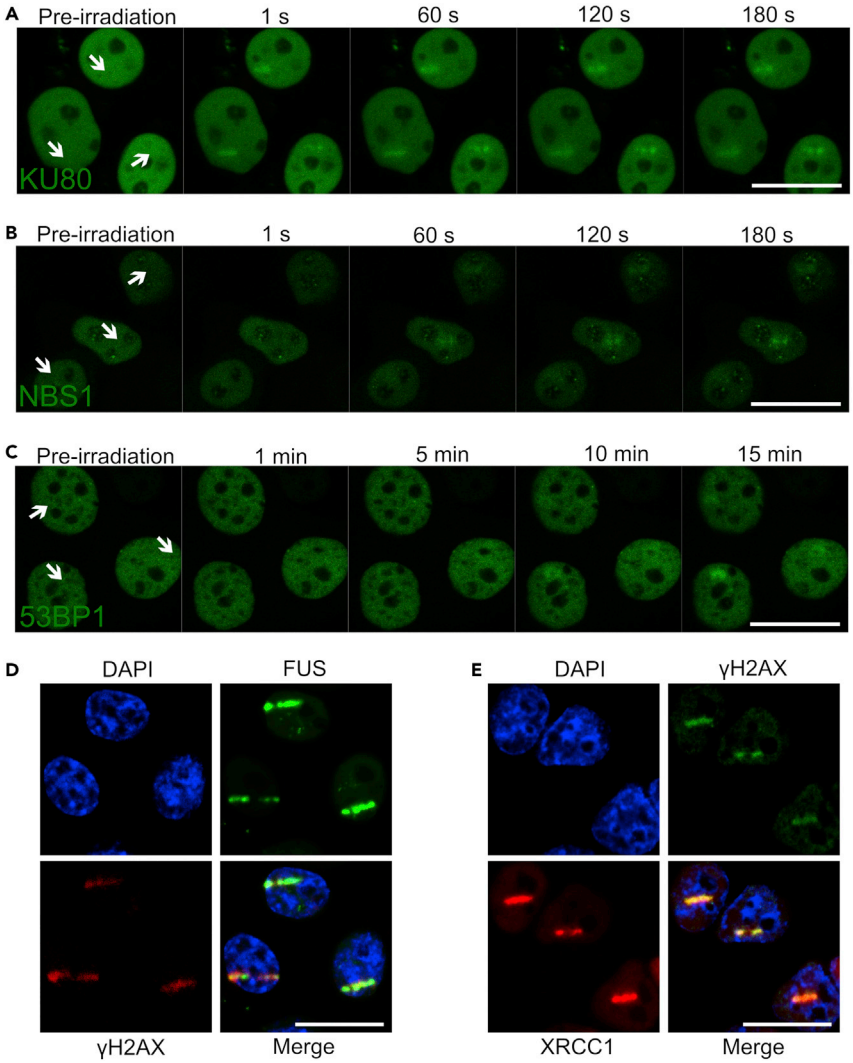

Figure 2. Representative recruitment of DNA damage repair-related proteins and validation steps

(A–C) Time course of recruitment of KU80-GFP, NBS1-GFP and 53BP1-GFP are respectively shown. The first image represents cells prior to irradiation, and following ones were taken at the indicated timepoints following irradiation. Arrows show the microirradiation site in each cell.

(D) FUS-GFP-transfected cells were irradiated, fixed with 4% PFA and stained with γH2AX (red).

(E) XRCC1-RFP-transfected cells were irradiated, fixed with 4% PFA and stained γH2AX (green). Scale: 20 μm.

We next microirradiated, fixed with 4% PFA, and stained HeLa cells transfected with XRCC1-RFP with γH2AX (green). XRCC1, a protein involved in DNA damage repair with major role on SSBs repair, co-localizes with DSBs sites (Figure 2E).

We have recently shown that the recruitment of key proteins to DNA damage sites is dependent on the liquid-liquid phase separation (LLPS), a critical process in the formation of biomolecular assemblies such as those implicated in the detection and the repair of DNA lesions (Levone et al., 2021; Pessina et al., 2019). To perform this protocol using drugs that affect the LLPS, the effect of these drug on phase separated membraneless nuclear organelles should be assessed for validation. We have previously assessed by immunofluorescence the effects of 50 μM ammonium acetate (Am. Ac.) and 2% 1,6-Hexanediol (1,6-HD) in Cajal bodies (CBs, coilin antibody) and nuclear speckles (NSs, SC-35 antibody). 2% 2,5-Hexanediol (2,5-HD) was used as a negative control. Figure 3A shows

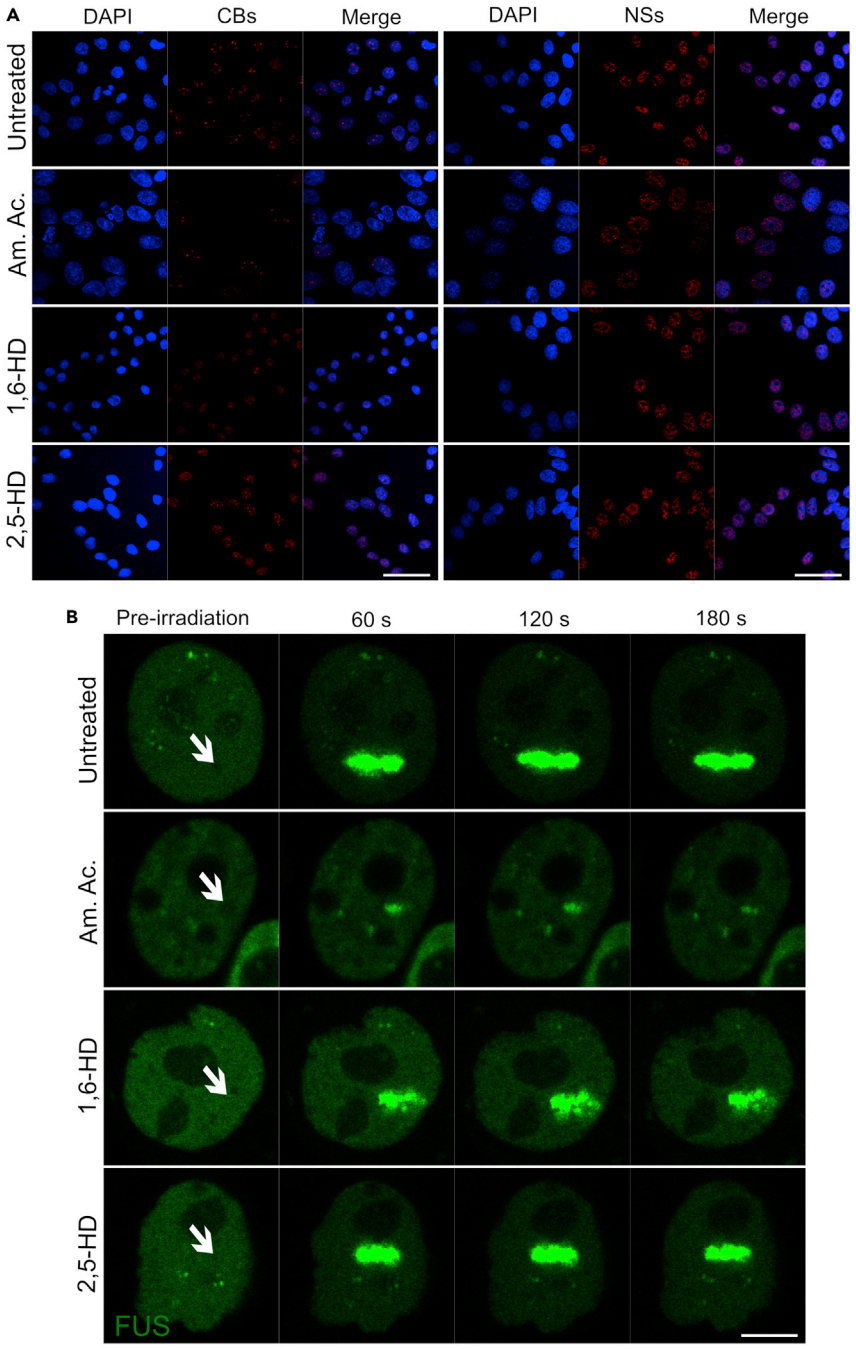

Figure 3. Example of the validation and laser microirradiation experiment using the drugs that disrupt the liquid–liquid phase separation (LLPS)

(A) HeLa cells were treated with either 50 μM ammonium acetate (Am. Ac.), 2% 1,6-Hexanediol (1,6-HD) or 2% 2,5-Hexanediol (2,5-HD, negative control), fixed after 30 min and stained with for Cajal Bodies (CBs, coilin antibody) or Nuclear Speckles (NSs, SC35 antibody). Am. Ac. and 1,6-HD disrupt almost all CBs, whereas NSs were disrupted to a lesser extent. 2,5-HD did not cause changes in these membraneless organelles. Scale: 40 μm.

(B) Time course of recruitment of FUS-GFP is shown. Arrows show the microirradiation site in each cell. While Am. Ac. and 1,6-HD reduced FUS recruitment to the laser microirradiation site, 2,5-HD caused minor effects. Scale: 5 μm.

that Am. Ac. and 1,6-HD disrupt almost all CBs, whereas NSs were disrupted to a lesser extent. 2,5-HD did not cause changes in these membraneless organelles. The aim of this validation is to find a treatment condition that is mild enough not to disrupt all subcellular structures, but at the same time strong enough to effectively disrupt LLPS. FUS is an RNA-binding proteins known to play roles on DNA damage repair (Levone et al., 2021; Mastrocola et al., 2013) and we recently showed that its recruitment to DNA damage sites is dependent on the LLPS. Figure 3B shows that while Am. Ac. and 1,6-HD reduced FUS recruitment to the laser microirradiation site, 2,5-HD caused minor effects. Using this experimental setting, it is possible to use the laser microirradiation protocol described here to assess whether the recruitment of any other protein to DNA damage site is dependent on the LLPS.

QUANTIFICATION AND STATISTICAL ANALYSIS

Once acquisition of irradiated cells is completed, exported data can be analyzed using Excel sheets. Figure 4 displays the exported data and the initial steps of analysis. As shown in Figure 1 (panel B), three ROIs are assigned to each cell, one in which irradiation occurred and two controls for the natural photobleaching due to successive photos being taken. To quantify the protein recruitment to the laser microirradiation sites, first subtract the fluorescence intensity of the background ROI from each individual ROI (irradiation ROI and each control ROI, Figure 4). Next, calculate the average of the three pre-irradiation images and then calculate the percentage of recruitment of each timepoint (fluorescence change post-irradiation), by multiplying their fluorescence intensity by 100 and dividing by the average of the fluorescence pre-irradiation for each ROI (which was used as normalizer, Figure 5). In Figure 5 it is possible to observe that while the fluorescence increases in the irradiation ROI (which represents the protein recruitment), it decreases in the control ROIs (which represents a bleaching due to sequential imaging). To take into consideration this bleaching, subtract the average of the respective control ROIs from the percentage of the irradiated ROI (see Figure 5) for each timepoint. The final formula used to calculate the protein recruitment is as follows:

$$\text{Recruitment (\%)} = \text{\% from baseline in irradiated ROI} - [(\text{\% from baseline in control ROI 1} + \text{\% from baseline in control ROI 2})/2]$$

Figure 6 displays an example of a recruitment graph made with Microsoft Excel, but other software or design could be used. To create the graph, time should be set as X axis and % recruitment as Y axis. The final result represents how much of the fluorescent protein accumulates at the DNA damage site, taking into account the pre-irradiation fluorescence, and the photobleaching due to sequential imaging. Figure 6 shows the dynamics of recruitment of transiently transfected FUS-GFP in HeLa cells, displaying one timepoint per second for a total of 3 min post-irradiation. It is possible to see that FUS is promptly recruited to laser microirradiation sites and remains there for all the time assessed, reaching a maximum of 600% recruitment, which means that the fluorescence intensity post-irradiation was 600 times higher than pre-irradiation (taking in consideration the normal photobleaching of the cells).

LIMITATIONS

Although this protocol is useful to study the recruitment of proteins to DNA damage, there are some limitations to be noted. The expression levels of the exogenous protein should be as close as possible to the endogenous one, as high protein expression could lead to non-physiological conditions and artifacts, such as protein aggregation or non-specific interactions with other proteins. Moreover, in the case of transiently transfected constructs, even if the level of expression is low enough to appreciate the recruitment of a given protein, the expression level differs among cells. For example, cells with high levels of protein expression should not be included in the experiment as a saturated fluorescence signal would cause an underestimation of the protein recruitment; on the other hand, low level of expression may cause an overestimation of the recruitment, if compared with other cells with higher expression which may reach saturation upon microirradiation.

	A	B	C	D	E	F	G	H	I	J	K	L
1			Cell 1			Cell 2			Cell 3			
2	Picture	Time [s]	Irradiation	Control 1	Control 2	Irradiation	Control 1	Control 2	Irradiation	Control 1	Control 2	Background
3	1	0.10	654.68	601.93	571.33	398.55	402.30	352.49	528.05	516.58	494.10	26.50
4	2	1.09	622.52	576.04	563.22	382.70	387.08	334.28	503.38	489.13	477.98	26.79
5	3	2.08	621.45	572.59	573.12	373.49	391.44	338.98	482.43	492.95	479.40	26.94
6	4	15.77	1084.05	541.16	501.95	458.78	381.62	309.59	459.53	504.45	469.99	27.03
7	5	16.76	1157.52	525.70	482.51	488.39	368.76	307.57	472.39	493.81	466.87	27.06
8	6	17.75	1210.85	525.80	489.50	516.74	369.10	305.83	471.98	481.15	461.89	27.26
9	7	18.75	1321.79	510.22	488.32	582.51	366.42	310.09	475.08	477.23	454.86	27.11
10	8	19.74	1390.30	525.68	475.69	649.96	364.12	297.94	515.93	483.58	461.04	27.17
11	9	20.73	1545.30	503.14	473.99	725.07	357.64	308.08	555.80	478.05	457.26	27.07
12	10	21.72	1673.83	510.65	467.93	813.53	357.32	307.82	570.92	479.49	461.84	27.35
13	11	22.71	1849.15	505.58	459.56	933.01	356.31	290.44	617.22	480.98	461.17	27.28
14	12	23.70	1953.40	487.64	446.66	1056.70	347.96	290.43	684.59	474.82	446.13	27.57
15	13	24.73	1996.57	494.86	446.39	1104.81	346.48	304.10	719.75	477.54	453.46	27.37
16	14	25.72	2114.70	494.71	460.98	1154.95	342.26	294.05	803.53	462.53	452.81	27.69
17	15	26.71	2170.59	487.64	456.50	1280.40	340.34	302.59	858.49	464.49	453.73	27.11
18	16	27.70	2230.81	500.35	450.50	1370.70	344.88	294.65	935.68	464.77	441.78	27.14
19	17	28.69	2212.28	497.05	442.79	1383.56	343.83	298.46	979.02	456.31	449.95	26.98
20	18	29.68	2320.68	497.44	447.33	1457.18	334.28	302.76	1052.96	447.07	446.71	27.38
21	19	30.67	2409.49	486.28	431.12	1509.65	340.76	292.07	1099.46	463.03	438.36	27.32
22	20	31.66	2581.92	490.91	422.82	1719.70	340.86	291.52	1210.58	444.77	431.85	27.22
23	21	32.66	2804.99	470.87	410.54	1896.72	326.72	288.50	1302.55	438.23	441.19	27.50
24	22	33.65	2834.91	454.07	404.07	1974.35	333.65	281.38	1315.52	433.52	438.83	27.16
25	23	34.63	2885.25	461.73	402.88	1937.20	323.75	285.77	1381.71	429.36	432.26	27.22
26	24	35.62	2910.51	448.19	419.70	1956.56	320.44	274.64	1430.04	426.20	437.97	27.32
27	25	36.61	2944.41	449.28	407.20	2078.38	331.97	274.02	1477.52	430.39	427.13	27.20
28	26	37.60	2851.48	464.70	410.55	2049.65	325.40	281.68	1561.40	427.52	437.74	26.95
29	27	38.59	2998.48	456.01	396.40	2149.94	310.70	282.25	1596.36	411.65	431.62	27.33
30	28	39.58	2993.19	441.31	397.29	2148.22	318.89	279.06	1615.67	418.00	424.19	27.01
31	29	40.58	3017.14	449.27	391.91	2256.34	314.07	270.98	1704.04	419.99	422.99	27.26
32	30	41.57	3045.75	447.67	399.22	2276.64	321.68	267.34	1719.13	410.55	422.62	27.59
33	31	42.56	3045.63	452.29	382.03	2293.98	307.19	278.82	1761.42	395.62	409.86	27.25
34	32	43.55	3071.15	435.48	385.28	2257.04	291.16	270.79	1797.19	405.63	410.44	27.44
35	33	44.55	3146.48	433.90	386.45	2296.86	293.42	265.74	1867.30	390.82	407.52	27.29
36	34	45.54	3127.17	429.74	386.57	2324.03	303.57	258.59	1911.36	393.95	406.10	27.15
37	35	46.53	3099.93	426.42	392.52	2349.36	295.44	275.93	1939.43	385.14	401.35	27.39
38	36	47.52	3191.46	420.51	374.26	2444.01	293.88	263.96	1979.67	380.01	400.64	27.34
39	37	48.51	3269.68	401.83	365.66	2638.18	289.60	265.76	2013.44	377.98	406.58	27.39
40	38	49.50	3411.11	406.48	363.30	2757.24	284.99	252.72	2060.20	374.59	401.97	27.19
41	39	50.50	3560.59	394.29	357.13	2874.44	288.51	254.29	2140.47	364.04	407.14	27.29
42	40	51.49	3637.41	392.13	353.85	2912.19	285.61	247.85	2160.33	355.69	388.19	27.24
43	41	52.48	3624.30	381.99	348.12	2983.92	281.79	244.99	2196.90	374.16	378.55	27.35
44	42	53.47	3588.21	384.64	353.70	2968.35	286.54	246.74	2242.19	362.96	392.38	27.47
45	43	54.45	3626.14	389.09	349.38	2923.65	283.04	251.27	2203.25	359.60	378.53	27.48
46	44	55.44	3600.04	390.65	346.34	2966.34	274.38	243.81	2194.27	346.37	379.91	27.14
47	45	56.43	3581.19	367.47	350.44	2865.31	278.42	235.77	2157.07	337.70	378.02	27.45
48	46	57.42	3539.29	388.10	347.06	2930.19	277.70	245.08	2208.21	345.69	365.58	27.54
49	47	58.42	3485.13	376.38	346.96	2890.47	275.94	239.51	2205.52	328.28	368.17	27.59
50	48	59.41	3605.05	389.86	342.04	2925.07	267.01	245.44	2255.11	342.73	363.57	27.47
51	49	60.40	3616.86	378.69	330.73	3087.75	273.28	239.37	2237.43	334.95	361.41	27.06
52	50	61.39	3758.87	367.72	336.04	3187.53	267.58	231.10	2299.72	329.56	368.71	27.48

Figure 4. Time measurement data exported into an Excel table and first steps of data processing

Column B shows the picture number and C represents the time of imaging. Pictures 1–3 (light yellow) are the acquisitions taken before microirradiation and 4 onward (dark yellow) are the acquisitions taken after microirradiation. Columns C–E, F–H and I–K show the fluorescence intensity of each cell (C, F and I display the fluorescence from irradiated ROIs and D–E, G–H and J–K display the fluorescence from control ROIs for each cell). Column L displays the background fluorescence. From each column (C–K), the background fluorescence should be subtracted.

	A	B	C	D	E	F	G	H
1	Picture	Irradiation	Control 1	Control 2	Irradiation	Control 1	Control 2	Recruitment
2					358.17	366.86	315.17	
3	1	372.05	375.80	325.99	103.88	102.44	103.43	0.94
4	2	355.91	360.29	307.49	99.37	98.21	97.56	1.48
5	3	346.55	364.50	312.04	96.76	99.36	99.01	-2.43
6	4	431.75	354.59	282.56	120.54	96.65	89.65	27.39
7	5	461.33	341.70	280.51	128.80	93.14	89.00	37.73
8	6	489.48	341.84	278.57	136.66	93.18	88.39	45.88
9	7	555.40	339.31	282.98	155.07	92.49	89.79	63.93
10	8	622.79	336.95	270.77	173.88	91.85	85.91	85.00
11	9	698.00	330.57	281.01	194.88	90.11	89.16	105.25
12	10	786.18	329.97	280.47	219.50	89.94	88.99	130.03
13	11	905.73	329.03	263.16	252.88	89.69	83.50	166.28
14	12	1029.13	320.39	262.86	287.33	87.33	83.40	201.96
15	13	1077.44	319.11	276.73	300.82	86.98	87.80	213.43
16	14	1127.26	314.57	266.36	314.73	85.75	84.51	229.60
17	15	1253.29	313.23	275.48	349.91	85.38	87.41	263.52
18	16	1343.56	317.74	267.51	375.12	86.61	84.88	289.37
19	17	1356.58	316.85	271.48	378.75	86.37	86.14	292.50
20	18	1429.80	306.90	275.38	399.20	83.66	87.37	313.68
21	19	1482.33	313.44	264.75	413.86	85.44	84.00	329.14
22	20	1692.48	313.64	264.30	472.54	85.49	83.86	387.86
23	21	1869.22	299.22	261.00	521.88	81.56	82.81	439.69
24	22	1947.19	306.49	254.22	543.65	83.54	80.66	461.55
25	23	1909.98	296.53	258.55	533.26	80.83	82.03	451.83
26	24	1929.24	293.12	247.32	538.64	79.90	78.47	459.45
27	25	2051.18	304.77	246.82	572.68	83.07	78.31	491.99
28	26	2022.70	298.45	254.73	564.73	81.35	80.82	483.64
29	27	2122.61	283.37	254.92	592.63	77.24	80.88	513.56
30	28	2121.21	291.88	252.05	592.24	79.56	79.97	512.47
31	29	2229.08	286.81	243.72	622.35	78.18	77.33	544.60
32	30	2249.05	294.09	239.75	627.93	80.16	76.07	549.81
33	31	2266.73	279.94	251.57	632.86	76.31	79.82	554.80
34	32	2229.60	263.72	243.35	622.50	71.89	77.21	547.95
35	33	2269.57	266.13	238.45	633.66	72.54	75.66	559.56
36	34	2296.88	276.42	231.44	641.28	75.35	73.43	566.89
37	35	2321.97	268.05	248.54	648.29	73.07	78.86	572.33
38	36	2416.67	266.54	236.62	674.73	72.65	75.08	600.86
39	37	2610.79	262.21	238.37	728.92	71.47	75.63	655.37
40	38	2730.05	257.80	225.53	762.22	70.27	71.56	691.31
41	39	2847.15	261.22	227.00	794.92	71.20	72.02	723.30
42	40	2884.95	258.37	220.61	805.47	70.43	70.00	735.26
43	41	2956.57	254.44	217.64	825.47	69.36	69.05	756.26
44	42	2940.88	259.07	219.27	821.08	70.62	69.57	750.99
45	43	2896.17	255.56	223.79	808.60	69.66	71.01	738.27
46	44	2939.20	247.24	216.67	820.62	67.39	68.75	752.55
47	45	2837.86	250.97	208.32	792.32	68.41	66.10	725.07
48	46	2902.65	250.16	217.54	810.41	68.19	69.02	741.81
49	47	2862.88	248.35	211.92	799.31	67.70	67.24	731.84
50	48	2897.60	239.54	217.97	809.00	65.29	69.16	741.77
51	49	3060.69	246.22	212.31	854.54	67.11	67.36	787.30
52	50	3160.05	240.10	203.62	882.28	65.45	64.61	817.25

Figure 5. Data analysis of a single cell

Columns B–D are the fluorescence intensity (with the background fluorescence already subtracted) for each ROI of a single cell. Pictures 1–3 (light yellow) were taken before microirradiation and are averaged in line 2 of columns E–G (orange). To calculate the percentage of recruitment, the fluorescence intensity of each timepoint was multiplied by 100 and divided by the average of the fluorescence pre-irradiation for each ROI (columns E–G, green, e.g., B3 * 100/E$2 or F50 * 100/F$2). It is possible to observe that while the fluorescence increases in the irradiation ROI (which represents the protein recruitment), it decreases in the control ROIs (which represents a bleaching due to sequential imaging). To take into consideration this natural bleaching, another normalization needs to be done (column H, blue, final relative recruitment). This was done by applying the following formula: Irradiation ROI – ((Control ROI 1 + Control ROI 2)/2), e.g., E3 – ((F3 + G3)/2). The sum of the three first timepoints in column H should always be 0, as these are the pre-irradiation points, and their average was used as normalizer.

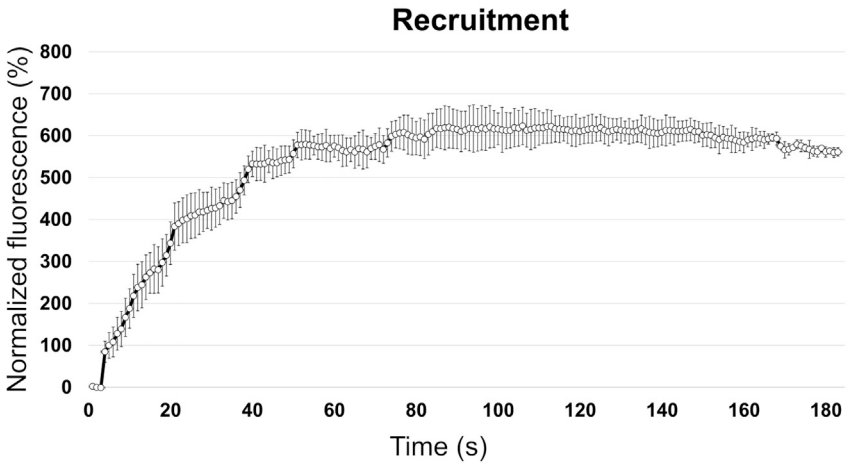

Figure 6. Representative graph displaying the recruitment of FUS-GFP in HeLa cells across time

While Figure 5 shows the calculation of FUS recruitment for a single cell, here we show the average FUS recruitment in five cells. Data are represented as mean ± SEM.

Another aspect that should be considered is that microirradiation with the 405 nm laser after Hoechst sensitization induces complex DNA lesions, not limited to double strand breaks (DSBs). Although a previous study found that 405 nm microirradiation of BrdU sensitized cells did not induce the formation of single strand breaks (SSBs) (Kong et al., 2009), us and others have recently found that SSBs are also generated (Gaudreau-Lapierre et al., 2018; Holton et al., 2017; Levone et al., 2021) by the microirradiation protocol using the 405 nm laser and Hoechst sensitization. This can easily be assessed by monitoring the recruitment of classical proteins involved in the sensing and repair of SSBs, such as XRCC1 and PARP1. Here, we show by immunofluorescence that XRCC1-RFP accumulates at laser microirradiation sites, colocalizing with γH2AX (Figure 2E).

In an experimental design, researchers using this protocol should microirradiate at least 10 cells per groups per replicate, and at least duplicates should be performed. Ensure that all replicates within one experiment use the same laser irradiation power, since it is directly proportional to the DNA damage extent. If the confocal setting to be used only permits the microirradiation of one cell at a time (or if the researcher has decided to proceed this way), this experiment can be very long and time consuming. Depending on the number of timepoints analyzed post-microirradiation, the final dataset produced may be very dense and a careful statistical analysis may be necessary, in case the difference between experimental groups is not clear. Besides that, for the immunofluorescence validation, finding the irradiated cells on a Petri dish may prove to be difficult; a grid to mark the irradiated cell may be used. Commercial gridded coverslips are also available and could be useful.

While working with drugs that disrupt LLPS, cell health is of concern, as these drugs may also impact other cellular processes, such as metabolism, signaling, etc. Finding a concentration that effectively disrupts phase separation without causing major impacts in cell viability is crucial for the experiments described here. The concentrations cited above worked for our experiments in HeLa cells, but adaptation may be necessary for different cell lines.

TROUBLESHOOTING

Problem 1

Cells look unhealthy.

Potential solution

Unhealthy cells (Figure 7A) could be due to the suboptimal transfection procedure or to cells having difficulty to completely attach to the glass slide. If cells are unhealthy before adding the Hoechst, the

transfection protocol could be optimized, or a glass coating (such as poly-D-lysine) could be applied. If cells are unhealthy after addition of LLPS drugs, the concentration used could be suboptimal and may need to be revised; if the lowest concentration that impact LLPS is already being used, try reducing the incubation time, e.g., 15 min rather than 30 min.

Problem 2

Cells move during image acquisition or cells change focus during image acquisition.

Potential solution

A focus stabilization is necessary. In case it is already active, focus change during acquisition could be due to cell movement or poor health (de-attaching). Cells with healthy morphology should be chosen for acquisition. If focus is lost during the process or the cell move too much (see Methods video S2), that cell should be excluded from the analysis.

Problem 3

Cells display variable expression levels.

Potential solution

This could be a problem because high expression could lead to a saturated signal and underestimation of protein recruitment. Try selecting cells with similar expression levels; cells with saturated signal (Figure 7B) or too low expression (Figure 7C) should not be used. If necessary, stably expressing cells could be used, or cells selection could be applied after transient transfection.

Problem 4

Cells display variable recruitment levels (Figure 7D).

Potential solution

This could occur because the protein recruitment to double strand breaks is dependent on the cell cycle. For example, BRCA1, a homologous recombination-related protein, is recruited predominantly when cells are in S/G2, and 53BP1, a nonhomologous end joining-related protein, is recruited predominantly when cells are in G1. Try synchronizing cells and assess only protein related to the cell cycle the cells are currently in.

Problem 5

Protein recruitment is not observed upon laser microirradiation.

Potential solution

First of all, this could mean that the protein is not recruited to the DNA damage sites. Perhaps it is recruited later on, or its recruitment is dependent on the cell cycle phase. To ensure that the assay works, it is important to establish the experimental setting using a positive control protein (such as KU80, NBS1, etc). If also the control protein is not recruited, this could be due to insufficient sensitization of the cells. Try using another sensitizer agent (such as BrdU) or increasing the laser irradiation power.

RESOURCE AVAILABILITY

Lead contact

Further information and requests for resources and reagents should be directed to and will be fulfilled by the lead contact, Prof. Silvia M. L. Barabino (silvia.barabino@unimib.it). Protocol-related questions should be directed to the technical contact, Dr. Brunno R. Levone (brunno.rochalevone@unimib.it).

Materials availability

The knockout cell lines used in this manuscript are available upon request. Some plasmids used are available at Addgene (KU80-GFP, Cat#46958; 53BP1-GFP, Cat#60813), or available upon request.

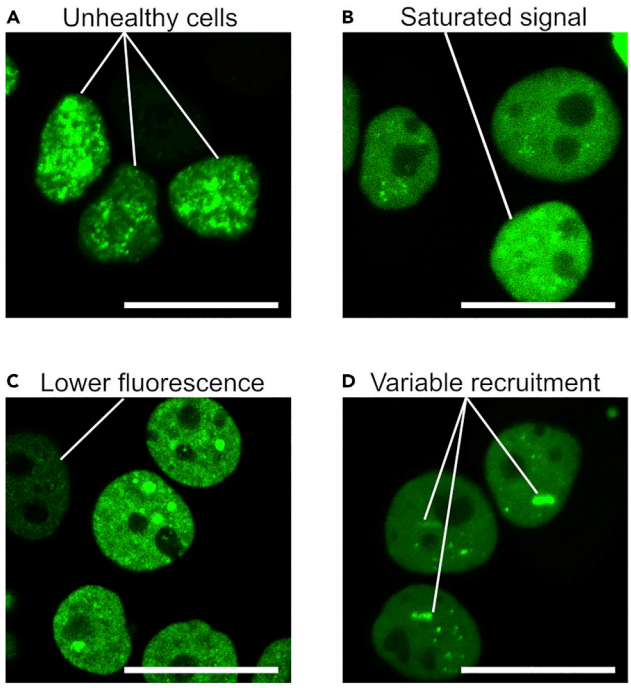

Figure 7. Troubleshoot, problems that could be encountered during microirradiation and image acquisition

All panels display FUS-GFP transfected HeLa cells.

(A) Cells display clusters of FUS-GFP, different from what is expected in healthy cells (see Figure 3B) and should not be used for the experiment. Cells displayed in all other panels are considered healthy cells.

(B) The indicated cell has a saturated fluorescence signal, which would generate unreliable data due to protein recruitment underestimation.

(C) The indicated cell has much lower fluorescence signal in comparison to all other cells (photo brightness was increased to better visualize the indicated cell), which would generate unreliable data due to overestimation of the protein recruitment.

(D) Cells with variable level of protein recruitment. Scale: 20 μm.

Data and code availability

This study did not generate datasets, but an example of analysis dataset with all formulas used here is available from the corresponding author on request.

SUPPLEMENTAL INFORMATION

Supplemental information can be found online at https://doi.org/10.1016/j.xpro.2022.101146.

ACKNOWLEDGMENTS

We thank Prof. Alessandra Agresti for technical support. The plasmid XRCC1-RFP was kindly provided by Prof. M. Cristina Cardoso (Department of Biology, Technical University of Darmstadt, Darmstadt, Germany). NBS1-GFP was kindly provided by Dr. A. Nussenzweig (Laboratory of Genome Integrity, National Institutes of Health, Bethesda, USA).

AUTHOR CONTRIBUTIONS

B.R.L. validated the microirradiation protocol and the analysis. B.R.L. and S.L. conducted the experiments. B.R.L. and S.L. wrote the paper. S.M.L.B. supervised the work and edited the manuscript.

DECLARATION OF INTERESTS

The authors declare no competing interests.

REFERENCES

Allodi, I., Comley, L., Nichterwitz, S., Nizzardo, M., Simone, C., Benitez, J.A., Cao, M., Corti, S., and Hedlund, E. (2016). Differential neuronal vulnerability identifies IGF-2 as a protective factor in ALS. Sci. Rep. *6*, 25960.

Babinchak, W.M., Dumm, B.K., Venus, S., Boyko, S., Putnam, A.A., Jankowsky, E., and Surewicz, W.K. (2020). Small molecules as potent biphasic modulators of protein liquid–liquid phase separation. Nat. Commun. *11*, 5574.

Britton, S., Coates, J., and Jackson, S.P. (2013). A new method for high-resolution imaging of Ku foci to decipher mechanisms of DNA double-strand break repair. J. Cell Biol. *202*, 579–595.

Fradet-Turcotte, A., Canny, M.D., Escribano-Diaz, C., Orthwein, A., Leung, C.C., Huang, H., Landry, M.C., Kitevski-Leblanc, J., Noordermeer, S.M., Sicheri, F., and Durocher, D. (2013). 53BP1 is a reader of the DNA-damage-induced H2A Lys 15 ubiquitin mark. Nature *499*, 50–54.

Gaudreau-Lapierre, A., Garneau, D., Djerir, B., Coulombe, F., Morin, T., and Marechal, A. (2018). Investigation of protein recruitment to DNA lesions using 405 Nm laser micro-irradiation. J. Vis. Exp. *133*, 57410.

Hamaguchi, M.S., Watanabe, K., and Hamaguchi, Y. (1997). Regulation of intracellular pH in sea urchin eggs by medium containing both weak acid and base. Cell Struct. Funct. *22* (4), 387–398.

Holton, N.W., Andrews, J.F., and Gassman, N.R. (2017). Application of laser micro-irradiation for examination of single and double strand break repair in mammalian cells. J. Vis. Exp. https://doi.org/10.3791/56265.

Jain, A., and Vale, R.D. (2017). RNA phase transitions in repeat expansion disorders. Nature *546* (7657), 243–247.

Kato, M., and McKnight, S.L. (2018). A Solid-State Conceptualization of Information Transfer from Gene to Message to Protein. Annu. Rev. Biochem. *87*, 351–390.

Kong, X., Mohanty, S.K., Stephens, J., Heale, J.T., Gomez-Godinez, V., Shi, L.Z., Kim, J.S., Yokomori, K., and Berns, M.W. (2009). Comparative analysis of different laser systems to study cellular responses to DNA damage in mammalian cells. Nucleic Acids Res. *37*, e68.

Kroschwald, S., Maharana, S., Mateju, D., Malinovska, L., Nüske, E., Poser, I., Richter, D., and Alberti, S. (2015). Promiscuous interactions and protein disaggregases determine the material state of stress-inducible RNP granules. eLife *4*, e06807.

Levone, B.R., Lenzken, S.C., Antonaci, M., Maiser, A., Rapp, A., Conte, F., Reber, S., Mechtersheimer, J., Ronchi, A.E., Muhlemann, O., et al. (2021). FUS-dependent liquid–liquid phase separation is important for DNA repair initiation. J. Cell Biol. *220*, e202008030.

Mastrocola, A.S., Kim, S.H., Trinh, A.T., Rodenkirch, L.A., and Tibbetts, R.S. (2013). The RNA-binding protein fused in sarcoma (FUS) functions downstream of poly(ADP-ribose) polymerase (PARP) in response to DNA damage. J. Biol. Chem. *288*, 24731–24741.

Mortusewicz, O., Roth, W., Li, N., Cardoso, M.C., Meisterernst, M., and Leonhardt, H. (2008). Recruitment of RNA polymerase II cofactor PC4 to DNA damage sites. J. Cell Biol. *183*, 769–776.

Muster, B., Rapp, A., and CARDOSO, M.C. (2017). Systematic analysis of DNA damage induction and DNA repair pathway activation by continuous wave visible light laser micro-irradiation. AIMS Genet. *4*, 47–68.

Pessina, F., Giavazzi, F., Yin, Y., Gioia, U., Vitelli, V., Galbiati, A., Barozzi, S., Garre, M., Oldani, A., Flaus, A., et al. (2019). Functional transcription promoters at DNA double-strand breaks mediate RNA-driven phase separation of damage-response factors. Nat. Cell Biol. *21*, 1286–1299.

Saquilabon Cruz, G.M., Kong, X., Silva, B.A., Khatibzadeh, N., Thai, R., Berns, M.W., and Yokomori, K. (2016). Femtosecond near-infrared laser microirradiation reveals a crucial role for PARP signaling on factor assemblies at DNA damage sites. Nucleic Acids Res. *44*, e27.

Tsukada, K., Shimada, M., Imamura, R., Saikawa, K., Ishiai, M., and Matsumoto, Y. (2021). The FHA domain of PNKP is essential for its recruitment to DNA damage sites and maintenance of genome stability. Mutat. Res. *822*, 111727.

Updike, D.L., Hachey, S.J., Kreher, J., and Strome, S. (2011). P granules extend the nuclear pore complex environment in the C. elegans germ line. J. Cell Biol. *192*, 939–948.

Yamazaki, T., Souquere, S., Chujo, T., Kobelke, S., Chong, Y.S., Fox, A.H., Bond, C.S., Nakagawa, S., Pierron, G., and Hirose, T. (2018). Functional Domains of NEAT1 Architectural lncRNA Induce Paraspeckle Assembly through Phase Separation. Mol. Cell. *70*, 1038–1053.e7.